HHS Public Access
Author manuscript
J Org Chem. Author manuscript; available in PMC 2021 May 25.

Published in final edited form as:
J Org Chem. 2020 February 07; 85(3): 1725–1730. doi:10.1021/acs.joc.9b02615.

PEGylation near a patch of non-polar surface residues increases the conformational stability of the WW domain

Steven R. E. Draper, **Dallin S. Ashton**, **Benjamin M. Conover**, **Anthony J. Carter**, **Kimberlee L. Stern**, **Qiang Xiao**, **Joshua L. Price**
Department of Chemistry and Biochemistry, Brigham Young University, Provo, Utah 84602, United States

Abstract

Many proteins have one or more surface-exposed patches of non-polar residues; our observations here suggest that PEGylation near such locations might be a useful strategy for increasing protein conformational stability. Specifically, we show that conjugating a PEG-azide to a propargyloxyphenylalanine via the copper (I)-catalyzed azide-alkyne cycloaddition can increase the conformational stability of the WW domain due to a favorable synergistic effect that depends on the hydrophobicity of a nearby patch of non-polar surface residues.

Graphical Abstract

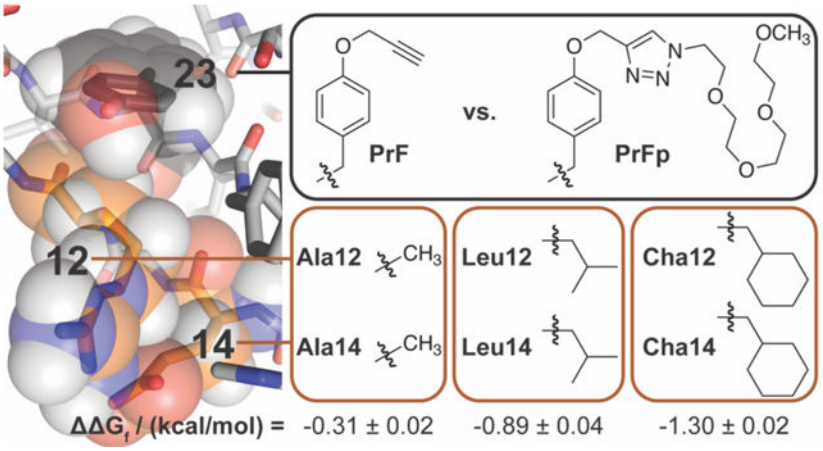

Modification of protein side chains with polyethylene glycol (PEG) has been used for more than thirty years to enhance the stability and pharmacokinetic properties of protein drugs.[1–8] Early efforts employed non-specific conjugation strategies that resulted in a heterogeneous mixture of PEGylated protein isoforms, which differed in the number and location of PEGylation sites; such strategies were easy to use, but frequently resulted in diminished stability and biological activity.[5] Powerful chemoselective side-chain modification chemistry now allows researchers to avoid PEGylation near enzyme active sites and protein binding

Supporting Information
Mass spectra, HPLC chromatograms, CD spectra, global fits of variable temperature CD data, and statistics for all fits.

interfaces,[9–16] but beyond this, there are few structure- or sequence-based guidelines for selecting PEGylation sites that optimally balance stability, pharmacokinetic benefits, and biological activity. We previously showed that the ability of a small PEGylated model protein to evade degradation by a cocktail of proteases depends strongly on the location of the PEGylation site, with the best sites characterized by the ability of PEG to increase protein conformational stability. Motivated by this observation, we seek to understand the molecular basis for PEG-based protein stabilization and to develop structure-based predictive guidelines for identifying optimal PEGylation sites.

The desolvation and burial of non-polar residues in the interior of protein tertiary and quaternary structures provides a major driving force for protein folding, via enthalpic and entropic contributions known collectively as the hydrophobic effect.[17–21] This process allows the ordered water molecules that surrounded the non-polar residues in the unfolded conformation to be released to bulk solvent upon folding; it also maximizes the contact surface area between non-polar side chains in the folded conformation. Previous observations suggest that side-chain PEGylation similarly releases surface bound water molecules in the immediate vicinity of the PEGylation site, thereby increasing protein conformational stability via an entropic effect.[22,23] We recently found that the strength of a salt bridge between Glu12 and Arg14 in the WW domain (hereafter called WW) increases when a propargyloxyphenylalanine residue at position 23 (PrF23) is modified with a PEG-azide via the copper-catalyzed azide-alkyne cycloaddition (compare **ER** vs **pER** in Table 1; Figure 1).[23] Presumably the resulting PEGylated PrF residue (PrFp23) strengthens the Glu12-Arg14 salt bridge by shielding it from interfering water molecules. Based on this observation, we wondered whether PrFp23 might be similarly able to shield or partially desolvate non-polar residues at positions 12 and 14, thereby increasing WW conformationally stability via the hydrophobic effect.

To test this hypothesis, we prepared WW variants **LL** and **pLL**, in which Leu occupies positions 12 and 14, with either PrF or PrFp, respectively at position 23 (one letter code: Z for PrF, Z̲ for PrFp). Variable temperature circular dichroism (CD) experiments reveal that **pLL** is −0.89 ± 0.04 kcal/mol more stable than non-PEGylated **LL** (Table 1). We used triple mutant box analysis[23–31] to explore the origins of this stabilizing effect by replacing Leu12 and/or Leu14 with Ala to generate variants **LA**, **AL**, and **AA**, along with their PEGylated counterparts **pLA**, **pAL**, and **pAA**. Comparing the folding free energies of these variants reveals that Leu12 and Leu14 engage in a favorable interaction in **pLL** ($\Delta\Delta\Delta G_f$ = −0.44 ± 0.04 kcal/mol, Table 2), but not in non-PEGylated **LL** ($\Delta\Delta\Delta G_f$ = −0.06 ± 0.05 kcal/mol, Table 2). PEGylation enhances the Leu12-Leu14 interaction by −0.38 ± 0.06 kcal/mol ($\Delta\Delta\Delta\Delta\Delta G_f$ in Table 2), a synergistic effect that represents a substantial fraction of the overall difference in stability between **pLL** and **LL** (see above). Based on this result, we wondered whether PEGylation of PrF23 would be similarly stabilizing for WW variants with other non-polar residues at positions 12 and 14, with more non-polar WW variants experiencing greater PEG-based stabilization.

To explore this possibility, we prepared and characterized additional derivatives of **LL** and **pLL**, in which Leu12 and/or Leu14 were replaced by Phe, Ala, or cyclohexylalanine (Cha; one-letter abbreviation is X) to give variants **FF**, **FA**, **AF**, **XX**, **XA**, **AX**, **XL**, **LX**, **FL**, and

LF, along with their PEGylated counterparts **pFF**, **pFA**, **pAF**, **pXX**, **pXA**, **pAX**, **pXL**, **pLX**, **pFL**, and **pLF**. We estimated the hydrophobicity of each side chain by calculating the logarithm of the water-octanol partition coefficient (c log P) of the corresponding N-acetyl amino acid N-methyl amide in ChemDraw; we calculated the overall hydrophobicity of residues 12 and 14 by averaging their individual c log P values. A plot of the impact of PEGylation on the folding free energy of each variant ($\Delta\Delta G_f$) vs. this composite c log P value is shown in Figure 2A. The data in these plots fit reasonably to a linear equation with a slope of −0.37 ± 0.07 kcal/mol per log unit ($R^2 = 0.70$), indicating that PEGylation at position 23 is more stabilizing when the residues that occupy positions 12 and 14 are more hydrophobic.

Next, we wondered whether these observations depended similarly on PEG-based strengthening of favorable synergistic interactions between residues at positions 12 and 14 as we observed above for **pLL**. Triple mutant box analysis of variant **pXX** (Table 2) reveals that PEGylation shifts the Cha12-Cha14 interaction from unfavorable ($\Delta\Delta\Delta G_f = 0.56 \pm 0.03$ kcal/mol) to favorable ($\Delta\Delta\Delta G_f = -0.41 \pm 0.04$ kcal/mol), a synergistic effect worth $\Delta\Delta\Delta\Delta G_f = -0.97 \pm 0.05$ kcal/mol. Similarly, PEG increases the strength of already favorable interactions between Cha12 and Leu14 in **pXL** and between Phe12 and Leu14 in **pFL** ($\Delta\Delta\Delta\Delta G_f = -0.39 \pm 0.06$ and -0.11 ± 0.05 kcal/mol, respectively). In contrast, PEGylation makes an unfavorable interaction in **pLF** between Leu12 and Phe14 less unfavorable ($\Delta\Delta\Delta\Delta G_f = -0.20 \pm 0.04$ kcal/mol) and has a destabilizing effect on the interaction between Phe12 and Phe14 in **pFF** ($\Delta\Delta\Delta\Delta G_f = 0.19 \pm 0.04$ kcal/mol). The variability among these $\Delta\Delta\Delta\Delta G_f$ values correlates inversely with the composite c log P values for residues 12 and 14 ($R^2 = 0.77$; slope = −0.67 ± 0.18 kcal/mol per log unit), indicating such that PEGylation better enhances the interaction between more hydrophobic residues (Figure 2B).

Many proteins have one or more surface-exposed patches of non-polar residues;[32] our observations here suggest that PEGylation near such locations might be a useful strategy for increasing protein conformational stability. Moreover, it is interesting that variants **pLL**, **pXX** and **pXL** (T_m = 61.9, 63.2, and 60.8 °C, respectively) are each more stable than the parent WW domain from which they were derived (T_m = 58.0 °C), highlighting the possibility of simultaneously engineering a PEGylation site and a nearby surface-exposed hydrophobic patch in place of native residues to achieve superior conformational stability relative to the native sequence.

Experimental Section

Peptide Synthesis.

WW variants **AA** and **pAA** were synthesized previously.[23] WW variants **AL**, **LA**, **LL**, **AF**, **FA**, **FF**, **XA**, **AX**, **XX**, **XL**, **FL**, and **LF** were prepared as the C-terminal acids via Fmoc-based solid-phase peptide synthesis on Fmoc-Gly-Wang resin (EMD Biosciences) as described previously.[22,23,33] Fmoc-protected amino acids with acid-labile side-chain protecting groups were purchased from Advanced ChemTech and used without further purification; we also used previously synthesized N-[(9H-Fluoren-9-ylmethoxy)-O-2-propyn-1yl-L-tyrosine.[33,34] Coupling reactions were carried out using 5 eq of the appropriate Fmoc-protected amino acid, 5 eq of 2-(1H-benzotriazole-1-yl)-1,1,3,3-

tetramethyluronium hexafluorophosphate (HBTU), 5 eq of N-hydroxybenzotriazole hydrate (HOBt), and 10 eq of N,N-diisopropylethylamine in N-methyl-2-pyrrolidinone (NMP). Fmoc deprotection reactions were carried out using 20% piperidine in N,N-dimethylformamide (DMF). Following the final deprotection step, WW variants **pAL**, **pLA**, **pLL**, **pAF**, **pFA**, **pFF**, **pXA**, **pAX**, **pXX**, **pXL**, **pFL**, and **pLF** were prepared from **AL**, **LA**, **LL**, **AF**, **FA**, **FF**, **XA**, **AX**, **XX**, **XL**, **FL**, and **LF** via on-resin copper (I) catalyzed azide-alkyne cycloaddition using previously synthesized PEG-azide 13-azido-2,5,8,11-tetraoxatridecane.[33,34]

WW variants were cleaved from resin and side-chain protecting groups were globally removed by stirring the resin for 2–4 hr in a solution of phenol (0.0625 g), water (62.5 μL), thioanisole (62.5 μL), ethanedithiol (31 μL) and triisopropylsilane (12.5 μL) in trifluoroacetic acid (TFA, 1 mL). The TFA solution was drained from the resin and proteins were precipitated by addition of diethyl ether (~40 mL). Following centrifugation, the ether was decanted and the pellet was dissolved in ~40 mL 1:1 water/acetonitrile, then was flash frozen over dry ice in acetone and lyophilized to remove volatile impurities. The resulting powder was stored at −20°C until purification.

Proteins were purified by preparative reverse-phase high performance liquid chromatography (HPLC) on a C18 column using a linear gradient of acetonitrile in water with 0.1% v/v TFA. Fractions containing the desired protein product were pooled, frozen, and lyophilized. Proteins were identified by electrospray ionization time of flight mass spectrometry (ESI-TOF); expected and observed exact masses appear below. Protein purity was assessed by analytical HPLC on a C18 column using a 10–60% gradient of acetonitrile in water with 0.1% v/v TFA over 50 min at a flow rate of 1 mL/min. Mass spectra and HPLC chromatograms for all peptides are available in the Supporting Information.

Variant **LL**. Molecular formula $C_{181}H_{273}N_{51}O_{48}S$; ESI-TOF MS: expected $[M+4H^+]/4$ = 991.2633; observed $[M+4H^+]/4$ = 991.2594. Retention time on analytical HPLC: 31.7 min.

Variant **LA**. Molecular formula $C_{178}H_{267}N_{51}O_{48}S$; ESI-TOF MS: expected $[M+4H^+]/4$ = 980.7516; observed $[M+4H^+]/4$ = 980.7500. Retention time on analytical HPLC: 36.2 min.

Variant **AL**. Molecular formula $C_{178}H_{267}N_{51}O_{48}S$; ESI-TOF MS: expected $[M+4H^+]/4$ = 980.7516; observed $[M+4H^+]/4$ = 980.7511. Retention time on analytical HPLC: 36.3 min.

Variant **pLL**. Molecular formula $C_{190}H_{292}N_{54}O_{52}S$; ESI-TOF MS: expected $[M+4H^+]/4$ = 1049.5477; observed $[M+4H^+]/4$ = 1049.5450. Retention time on analytical HPLC: 28.2 min.

Variant **pLA**. Molecular formula $C_{187}H_{286}N_{54}O_{52}S$; ESI-TOF MS: expected $[M+4H^+]/4$ = 1039.0360; observed $[M+4H^+]/4$ = 1039.0326. Retention time on analytical HPLC: 35.7 min.

Variant **pAL**. Molecular formula $C_{187}H_{286}N_{54}O_{52}S$; ESI-TOF MS: expected $[M+4H^+]/4$ = 1039.0360; observed $[M+4H^+]/4$ = 1039.0357. Retention time on analytical HPLC: 35.5 min.

Variant **FF**. Molecular formula $C_{187}H_{269}N_{51}O_{48}S$; ESI-TOF MS: expected $[M+4H^+]/4$ = 1008.2555; observed $[M+4H^+]/4$ = 1008.2572. Retention time on analytical HPLC: 46.0 min.

Variant **FA**. Molecular formula $C_{181}H_{265}N_{51}O_{48}S$; ESI-TOF MS: expected $[M+4H^+]/4$ = 989.2476; observed $[M+4H^+]/4$ = 989.2472. Retention time on analytical HPLC: 40.3 min.

Variant **AF**. Molecular formula $C_{181}H_{265}N_{51}O_{48}S$; ESI-TOF MS: expected $[M+4H^+]/4$ = 989.2476; observed $[M+4H^+]/4$ = 989.2480. Retention time on analytical HPLC: 42.3 min.

Variant **pFF**. Molecular formula $C_{196}H_{288}N_{54}O_{52}S$; ESI-TOF MS: expected $[M+4H^+]/4$ = 1066.5399; observed $[M+4H^+]/4$ = 1066.5338. Retention time on analytical HPLC: 30.4 min.

Variant **pFA**. Molecular formula $C_{190}H_{284}N_{54}O_{52}S$; ESI-TOF MS: expected $[M+4H^+]/4$ = 1047.5321; observed $[M+4H^+]/4$ = 1047.5375. Retention time on analytical HPLC: 33.2 min.

Variant **pAF**. Molecular formula $C_{190}H_{284}N_{54}O_{52}S$; ESI-TOF MS: expected $[M+4H^+]/4$ = 1047.5321; observed $[M+4H^+]/4$ = 1047.5337. Retention time on analytical HPLC: 24.4 min.

Variant **XX**. Molecular formula $C_{187}H_{281}N_{51}O_{48}S$; ESI-TOF MS: expected $[M+4H^+]/4$ = 1011.2790; observed $[M+4H^+]/4$ = 1011.2825. Retention time on analytical HPLC: 36.2 min.

Variant **XA**. Molecular formula $C_{181}H_{271}N_{51}O_{48}S$; ESI-TOF MS: expected $[M+4H^+]/4$ = 990.7594; observed $[M+4H^+]/4$ = 990.7580. Retention time on analytical HPLC: 37.7 min.

Variant **AX**. Molecular formula $C_{181}H_{271}N_{51}O_{48}S$; ESI-TOF MS: expected $[M+4H^+]/4$ = 990.7594; observed $[M+4H^+]/4$ = 990.7629. Retention time on analytical HPLC: 37.7 min.

Variant **pXX**. Molecular formula $C_{196}H_{300}N_{54}O_{52}S$; ESI-TOF MS: expected $[M+4H^+]/4$ = 1069.5634; observed $[M+4H^+]/4$ = 1069.5557. Retention time on analytical HPLC: 32.8 min.

Variant **pXA**. Molecular formula $C_{190}H_{290}N_{54}O_{52}S$; ESI-TOF MS: expected $[M+4H^+]/4$ = 1049.0438; observed $[M+4H^+]/4$ = 1049.0425. Retention time on analytical HPLC: 36.8 min.

Variant **pAX**. Molecular formula $C_{190}H_{290}N_{54}O_{52}S$; ESI-TOF MS: expected $[M+4H^+]/4$ = 1049.0438; observed $[M+4H^+]/4$ = 1049.0381. Retention time on analytical HPLC: 37.4 min.

Variant **XL**. Molecular formula $C_{184}H_{277}N_{51}O_{48}S$; ESI-TOF MS: expected $[M+4H^+]/4$ = 1001.2711; observed $[M+4H^+]/4$ = 1001.2705. Retention time on analytical HPLC: 38.9 min.

Variant **FL**. Molecular formula $C_{184}H_{271}N_{51}O_{48}S$; ESI-TOF MS: expected $[M+4H^+]/4$ = 999.7594; observed $[M+4H^+]/4$ = 999.7586. Retention time on analytical HPLC: 37.7 min.

Variant **LF**. Molecular formula $C_{184}H_{271}N_{51}O_{48}S$; ESI-TOF MS: expected $[M+4H^+]/4$ = 999.7594; observed $[M+4H^+]/4$ = 999.7577. Retention time on analytical HPLC: 37.9 min.

Variant **pXL**. Molecular formula $C_{193}H_{296}N_{54}O_{52}S$; ESI-TOF MS: expected $[M+4H^+]/4$ = 1059.5555; observed $[M+4H^+]/4$ = 1059.5534. Retention time on analytical HPLC: 38.3 min.

Variant **pFL**. Molecular formula $C_{193}H_{290}N_{54}O_{52}S$; ESI-TOF MS: expected $[M+4H^+]/4$ = 1058.0438; observed $[M+4H^+]/4$ = 1058.0419. Retention time on analytical HPLC: 36.5 min.

Variant **pLF**. Molecular formula $C_{193}H_{290}N_{54}O_{52}S$; ESI-TOF MS: expected $[M+4H^+]/4$ = 1058.0438; observed $[M+4H^+]/4$ = 1058.0412. Retention time on analytical HPLC: 37.1 min.

CD Measurements.

Measurements were made with an Aviv 420 Circular Dichroism Spectropolarimeter, using quartz cuvettes with a path length of 0.1 cm. Solutions of each WW variant were prepared in 20 mM sodium phosphate buffer, pH 7; solution concentrations were determined spectroscopically based on tyrosine and tryptophan absorbance at 280 nm in 6 M guanidine hydrochloride + 20 mM sodium phosphate (ε_{Trp} = 5690 $M^{-1}cm^{-1}$, ε_{Tyr} = 1280 $M^{-1}cm^{-1}$).[35] CD spectra of 50 μM solutions were obtained from 260 to 200 nm at 25°C.

Variable temperature CD data were obtained at least in triplicate (one sample was made and then aliquoted into three different cuvettes) by monitoring the molar ellipticity [θ] at 227 nm of 50 μM solutions of each WW variant in 20 mM sodium phosphate (pH 7) from 1 to 95 °C, at 2 °C intervals, with 120 s equilibration time between data points and 30 s averaging time. Triplicate variable temperature CD data for each peptide were fit globally to a two-state model for thermally induced unfolding. We used nonlinear least-squares regression to fit the three data sets globally to equations derived from the two-state folding model of folding for each variant to obtain a melting temperature T_m and temperature-dependent folding free energy ΔG_f for each variant, as described in detail in the Supporting Information, which also contains statistics for the fits, including R^2 and sum of the square residuals.

Supplementary Material

Refer to Web version on PubMed Central for supplementary material.

Acknowledgements

This work was supported by National Institutes of Health Grant R15 GM116055-01.

References

(1). Abuchowski A; Vanes T; Palczuk NC; Davis FF “Alteration of Immunological Properties of Bovine Serum-Albumin by Covalent Attachment of Polyethylene-Glycol.”J. Biol. Chem 1977, 252, 3578. [PubMed: 405385]

(2). Abuchowski A; Mccoy JR; Palczuk NC; Vanes T; Davis FF “Effect of Covalent Attachment of Polyethylene-Glycol on Immunogenicity and Circulating Life of Bovine Liver Catalase.”J. Biol. Chem 1977, 252, 3582. [PubMed: 16907]

(3). Harris JM; Chess RB “Effect of pegylation on pharmaceuticals.”Nat. Rev. Drug Discov 2003, 2, 214. [PubMed: 12612647]

(4). Frokjaer S; Otzen DE “Protein drug stability: A formulation challenge.”Nat Rev Drug Discov 2005, 4, 298. [PubMed: 15803194]

(5). Fishburn CS “The pharmacology of PEGylation: Balancing PD with PK to generate novel therapeutics.”J. Pharm. Sci 2008, 97, 4167. [PubMed: 18200508]

(6). Veronese FM; Mero A “The Impact of PEGylation on Biological Therapies.”Biodrugs 2008, 22, 315. [PubMed: 18778113]

(7). PEGylated Protein Drugs: Basic Sience and Clinical Applications; Veronese FM, Ed.; Birkhauser Verlag: Basel, 2009.

(8). Jevsevar S; Kunstelj M; Porekar VG “PEGylation of therapeutic proteins.”Biotechnol. J 2010, 5, 113. [PubMed: 20069580]

(9). Dawson PE; Kent SBH “SYNTHESIS OF NATIVE PROTEINS BY CHEMICAL LIGATION 1.”Annu. Rev. Biochem 2000, 69, 923. [PubMed: 10966479]

(10). Rosendahl MS; Doherty DH; Smith DJ; Carlson SJ; Chlipala EA; Cox GN “A Long-Acting, Highly Potent Interferon α-2 Conjugate Created Using Site-Specific PEGylation.”Bioconjugate Chem. 2005, 16, 200.

(11). Dirksen A; Dawson PE “Expanding the scope of chemoselective peptide ligations in chemical biology.”Curr. Opin. Chem. Biol 2008, 12, 760—766. [PubMed: 19058994]

(12). Brocchini S; Godwin A; Balan S; Choi J.-w.; Zloh M; Shaunak S “Disulfide bridge based PEGylation of proteins.”Adv. Drug Deliv. Rev 2008, 60, 3. [PubMed: 17920720]

(13). Van de Vijver P; Suylen D; Dirksen A; Dawson PE; Hackeng TM “N-epsilon-(Thiaprolyl)-lysine as a Handle for Site-Specific Protein Conjugation.” Biopolymers 2010, 94, 465. [PubMed: 20593461]

(14). Cho H; Daniel T; Buechler YJ; Litzinger DC; Maio Z; Putnam AM; Kraynov VS; Sim BC; Bussell S; Javahishvili T; Kaphle S; Viramontes G; Ong M; Chu S; Becky GC; Lieu R; Knudsen N; Castiglioni P; Norman TC; Axelrod DW; Hoffman AR; Schultz PG; DiMarchi RD; Kimmel BE “Optimized clinical performance of growth hormone with an expanded genetic code.”Proc. Natl. Acad. Sci. USA 2011, 108, 9060. [PubMed: 21576502]

(15). Tada S; Andou T; Suzuki T; Dohmae N; Kobatake E; Ito Y “Genetic PEGylation.”Plos One 2012, 7, e49235. [PubMed: 23145132]

(16). Levine PM; Craven TW; Bonneau R; Kirshenbaum K “Semisynthesis of Peptoid-Protein Hybrids by Chemical Ligation at Serine.”Org. Lett 2014, 16, 512. [PubMed: 24393000]

(17). Nicholls A; Sharp KA; Honig B “Protein folding and association: insights from the interfacial and thermodynamic properties of hydrocarbons.”Proteins 1991, 11, 281. [PubMed: 1758883]

(18). Lins L; Brasseur R “The hydrophobic effect in protein folding.”FASEB J. 1995, 9, 535. [PubMed: 7737462]

(19). Dill KA “The Meaning of Hydrophobicity.”Science 1990, 250, 297. [PubMed: 2218535]

(20). Dill KA “Dominant Forces in Protein Folding.”Biochemistry 1990, 29, 7133. [PubMed: 2207096]

(21). Dill KA; Bromberg S; Yue KZ; Fiebig KM; Yee DP; Thomas PD; Chan HS “Principles of Protein-Folding - a Perspective from Simple Exact Models.”Protein Sci. 1995, 4, 561. [PubMed: 7613459]

(22). Lawrence PB; Gavrilov Y; Matthews SS; Langlois MI; Shental-Bechor D; Greenblatt HM; Pandey BK; Smith MS; Paxman R; Torgerson CD; Merrell JP; Ritz CC; Prigozhin MB; Levy Y;

Price JL “Criteria for Selecting PEGylation Sites on Proteins for Higher Thermodynamic and Proteolytic Stability.”J. Am. Chem. Soc 2014, 136, 17547. [PubMed: 25409346]

(23). Xiao Q; Draper SRE; Smith MS; Brown N; Pugmire NAB; Ashton DS; Carter AJ; Lawrence EEK; Price JL “Influence of PEGylation on the Strength of Protein Surface Salt Bridges.”ACS Chem. Biol 2019, 14, 1652. [PubMed: 31188563]

(24). Horovitz A; Fersht AR “Strategy for Analyzing the Cooperativity of Intramolecular Interactions in Peptides and Proteins.”J. Mol. Biol 1990, 214, 613. [PubMed: 2388258]

(25). Luisi DL; Snow CD; Lin JJ; Hendsch ZS; Tidor B; Raleigh DP “Surface salt bridges, double-mutant cycles, and protein stability: an experimental and computational analysis of the interaction of the Asp 23 side chain with the N-terminus of the N-terminal domain of the ribosomal protein L9.”Biochemistry 2003, 42, 7050. [PubMed: 12795600]

(26). Price JL; Powers DL; Powers ET; Kelly JW “Glycosylation of the Enhanced Aromatic Sequon is Similarly Stabilizing in Three Distinct Reverse Turn Contexts.”Proc. Natl. Acad. Sci. USA 2011, 108, 14127. [PubMed: 21825145]

(27). Price JL; Powers ET; Kelly JW “N-PEGylation of a Reverse Turn is Stabilizing in Multiple Sequence Contexts unlike N-GlcNAcylation.”ACS Chem. Biol 2011, 6, 1188. [PubMed: 21939258]

(28). Smith MS; Billings WM; Whitby FG; Miller MB; Price JL “Enhancing a long-range salt bridge with intermediate aromatic and nonpolar amino acids.”Org. Biomol. Chem 2017, 15, 5882. [PubMed: 28678274]

(29). Chao SH; Matthews SS; Paxman R; Aksimentiev A; Gruebele M; Price JL “Two Structural Scenarios for Protein Stabilization by PEG.”J. Phys. Chem. B 2014, 118, 8388. [PubMed: 24821319]

(30). Pandey BK; Enck S; Price JL “Stabilizing Impact of N-Glycosylation on the WW Domain Depends Strongly on the Asn-GlcNAc Linkage.”ACS Chem. Biol 2013, 8, 2140. [PubMed: 23937634]

(31). Chen WT; Enck S; Price JL; Powers DL; Powers ET; Wong CH; Dyson HJ; Kelly JW “Structural and Energetic Basis of Carbohydrate-Aromatic Packing Interactions in Proteins.”J Am Chem Soc 2013, 135, 9877. [PubMed: 23742246]

(32). Lijnzaad P; Berendsen HJ; Argos P “Hydrophobic patches on the surfaces of protein structures.” Proteins 1996, 25, 389. [PubMed: 8844873]

(33). Draper SRE; Lawrence PB; Billings WM; Xiao Q; Brown NP; Becar NA; Matheson DJ; Stephens AR; Price JL “Polyethylene Glycol Based Changes to beta-Sheet Protein Conformational and Proteolytic Stability Depend on Conjugation Strategy and Location.”Bioconjugate Chem. 2017, 28, 2507.

(34). Lawrence PB; Billings WM; Miller MB; Pandey BK; Stephens AR; Langlois MI; Price JL “Conjugation Strategy Strongly Impacts the Conformational Stability of a PEG-Protein Conjugate.”ACS Chem. Biol 2016, 11, 1805. [PubMed: 27191252]

(35). Edelhoch H “Spectroscopic Determination of Tryptophan and Tyrosine in Proteins.”Biochemistry 1967, 6, 1948. [PubMed: 6049437]

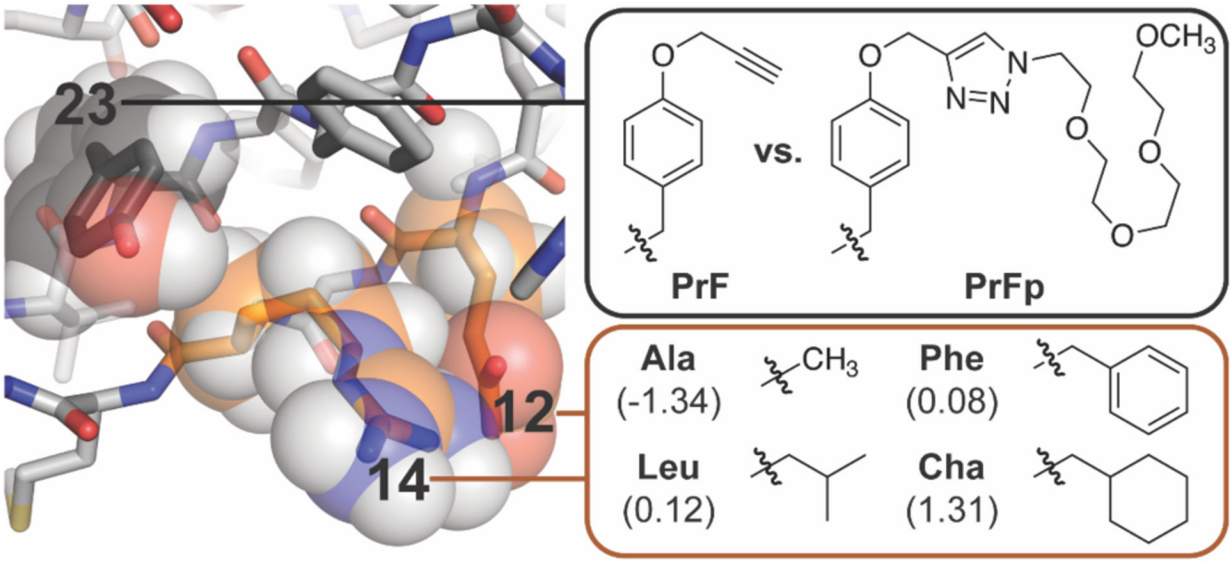

Figure 1.

Ribbon diagram of the parent WW domain (PDB ID: 1PIN) from which the variants described here were derived. The orange outlined box shows the non-polar residues that we incorporated at positions 12 and 14, which are highlighted in orange space-filling spheres. Shown in parentheses are the c log P values for the corresponding N-acetyl N-methyl amino acid amide. The black outlined box shows the PrF and PrFp residues that we incorporated at position 23, which is highlighted in black space-filling spheres.

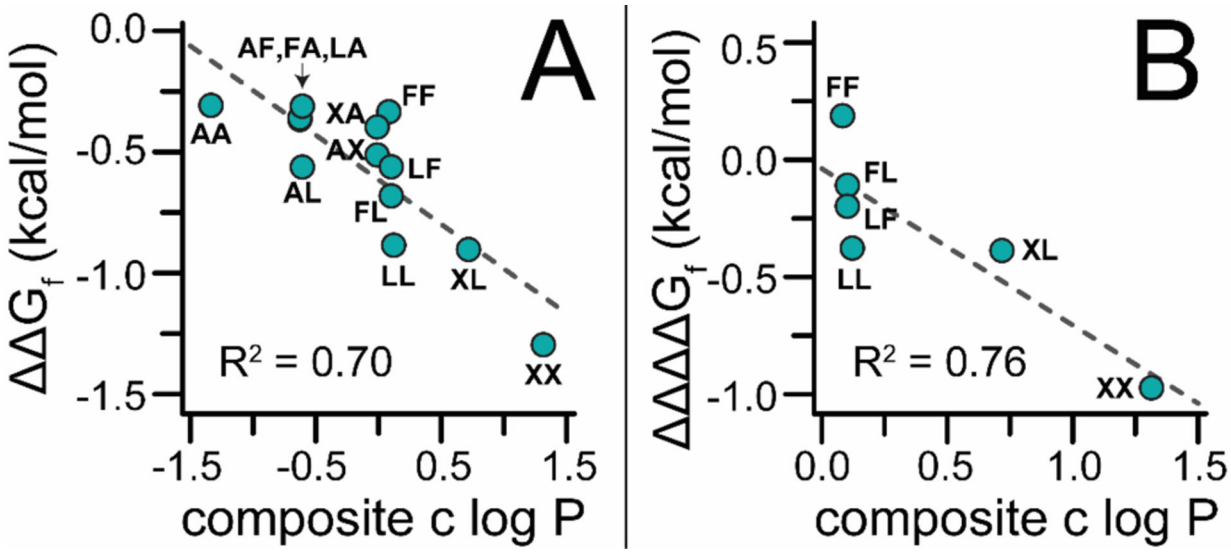

Figure 2.

(A) Plot of the impact of PrF-PEGylation at position 23 the conformational stability of WW variants **pAA**, p**LA**, **pAL**, **pLL**, **pFA**, **pAF**, **pFF**, **pXA**, **pAX**, **pXX**, **pXL**, **pFL**, and **pLF** relative to their non-PEGylated counterparts ($\Delta\Delta G_f$) vs. the composite c log P for residues at positions 12 and 14. Dotted line is a fit of the data to a linear equation with the indicated R^2 value. (B) Plot of the impact of PrF-PEGylation on the synergistic interaction between residues 12 and 14 ($\Delta\Delta\Delta\Delta G_f$) in variants **pLL**, **pFF**, **pXX**, **pXL**, **pFL**, and **pLF** vs. the composite c log P values for residues at these positions. Dotted line is a fit of the date to a linear equation with the indicated R^2 value.

Table 1.

Sequences, melting temperatures and folding free energy changes of PEGylated WW variants relative to their non-PEGylated counterparts.[a]

Peptide	Sequence	T_m (^{0}C)	$\Delta\Delta G_f$ (kcal/mol)
WW	KLPPGWEKRMSRSSGRVYYFNHITNASQFERPSG	58.0	
ER	••••••••••••••••••Z••••••••••••••••	51.9	
pER	••••••••••••••••••Z••••••••••••••••	55.6	-0.30 ± 0.03
LL	••••••L•L••••••••Z••••••••••••••••	52.0	
pLL	••••••L•L••••••••Z••••••••••••••••	61.9	-0.89 ± 0.04
LA	••••••L•A••••••••Z••••••••••••••••	51.8	
pLA	••••••L•A••••••••Z••••••••••••••••	55.3	-0.31 ± 0.02
AL	••••••A•L••••••••Z••••••••••••••••	42.1	
pAL	••••••A•L••••••••Z••••••••••••••••	48.4	-0.56 ± 0.04
AA	••••••A•A••••••••Z••••••••••••••••	42.8	
pAA	••••••A•A••••••••Z••••••••••••••••	46.5	-0.31 ± 0.02
FF	••••••F•F••••••••Z••••••••••••••••	50.7	
pFF	••••••F•F••••••••Z••••••••••••••••	54.7	-0.33 ± 0.02
FA	••••••F•A••••••••Z••••••••••••••••	43.8	
pFA	••••••F•A••••••••Z••••••••••••••••	48.5	-0.36 ± 0.02
AF	••••••A•F••••••••Z••••••••••••••••	51.2	
pAF	••••••A•F••••••••Z••••••••••••••••	55.5	-0.37 ± 0.02
XX	••••••X•X••••••••Z••••••••••••••••	49.2	
pXX	••••••X•X••••••••Z••••••••••••••••	63.2	-1.30 ± 0.02
XA	••••••X•A••••••••Z••••••••••••••••	43.2	
pXA	••••••X•A••••••••Z••••••••••••••••	47.8	-0.40 ± 0.02
AX	••••••A•X••••••••Z••••••••••••••••	52.3	
pAX	••••••A•X••••••••Z••••••••••••••••	58.4	-0.51 ± 0.02
XL	••••••X•L••••••••Z••••••••••••••••	49.9	
pXL	••••••X•L••••••••Z••••••••••••••••	60.8	-0.90 ± 0.02
FL	••••••F•L••••••••Z••••••••••••••••	46.9	
pFL	••••••F•L••••••••Z••••••••••••••••	55.5	-0.68 ± 0.02
LF	••••••L•F••••••••Z••••••••••••••••	48.2	
pLF	••••••L•F••••••••Z••••••••••••••••	55.5	-0.56 ± 0.02

[a] **X** = cyclohexylalanine (Cha), **Z** = propargyloxyphenylalanine (PrF); **Z** = PrFPEG. $\Delta\Delta G_f$ value for each PEGylated variant is given ± standard error relative to its non-PEGylated counterpart in kcal/mol at 50 μM protein concentration, in 20 mM sodium phosphate buffer (pH 7), at the melting temperature of the non-PEGylated protein. Data for **WW** are from reference 22. Data for variants **ER** and **pER** are from reference 23.

Table 2.

Triple mutant box analysis of the impact of PEGylation the interaction between residues 12 and 14 within variants **pLL**, **pFF**, **pXX**, **pXL**, **pFL** and **pLF**.[a]

Peptide	ΔG_f (kcal/mol)	$\Delta\Delta\Delta G_f$[b] (kcal/mol)	$\Delta\Delta\Delta\Delta G_f$[c] (kcal/mol)
AA	0.60 ± 0.02		
LA	−0.12 ± 0.02		
AL	0.61 ± 0.04		
LL	−0.17 ± 0.02	−0.06 ± 0.05	
pAA	0.30 ± 0.01		
pLA	−0.46 ± 0.01		
pAL	0.15 ± 0.02		
pLL	−1.05 ± 0.02	−0.44 ± 0.03	−0.38 ± 0.06
AA	0.53 ± 0.02		
FA	0.44 ± 0.02		
AF	−0.16 ± 0.01		
FF	−0.19 ± 0.02	0.06 ± 0.03	
pAA	0.22 ± 0.01		
pFA	0.05 ±0.01		
pAF	−0.53 ±0.01		
pFF	−0.46 ±0.01	0.25 ± 0.02	0.19 ± 0.04
AA	0.63 ± 0.02		
XA	0.42 ±0.01		
AX	−0.16 ±0.02		
XX	0.19 ±0.02	0.56 ± 0.03	
pAA	0.33 ± 0.01		
pXA	0.23 ± 0.03		
pAX	−0.67 ± 0.02		
pXX	−1.18 ± 0.01	−0.41 ± 0.04	−0.97 ± 0.05
AA	0.40 ± 0.02		
XA	0.26 ± 0.01		
AL	0.43 ± 0.03		
XL	−0.24 ±0.01	−0.53 ± 0.04	
pAA	0.10 ± 0.01		
pXA	−0.01 ±0.03		
pAL	−0.07 ± 0.02		
pXL	−1.09 ±0.02	−0.91 ± 0.04	−0.39 ± 0.06
AA	0.33 ±0.02		
FA	0.25 ± 0.02		
AL	0.43 ± 0.03		
FL	−0.01 ±0.02	−0.28 ± 0.04	
pAA	0.02 ± 0.01		

Peptide	ΔG_f (kcal/mol)	$\Delta\Delta\Delta G_f$ [b] (kcal/mol)	$\Delta\Delta\Delta\Delta G_f$ [c] (kcal/mol)
pFA	−0.13 ± 0.01		
pAL	−0.14 ± 0.02		
pFL	−0.69 ± 0.01	−0.39 ± 0.03	−0.11 ± 0.05
AA	0.66 ± 0.02		
LA	−0.06 ± 0.02		
AF	−0.03 ± 0.02		
LF	0.23 ± 0.01	0.99 ± 0.03	
pAA	0.36 ± 0.01		
pLA	−0.39 ± 0.01		
pAF	−0.40 ± 0.01		
pLF	−0.36 ± 0.01	0.79 ± 0.03	−0.20 ± 0.04

[a] ΔG_f, $\Delta\Delta\Delta G_f$, and $\Delta\Delta\Delta\Delta G_f$ values are given ± standard error. ΔG_f values for each of the eight peptides within the same triple mutant box were calculated at their average melting temperature: 323.3 K for **pLL** and its derivatives; 322.3 K for **pFF** and its derivatives; 323.5 K for **pXX** and its derivatives; 320.8 K for **pXL** and its derivatives; 320.0 K for **pFL** and its derivatives; 324.0 K for **pLF** and its derivatives. Because variants **AA**, **AL**, **LA**, **AF**, **FA**, and **XA** and their PEGylated counterparts appear in more than one triple mutant box, their ΔG_f values are necessarily presented at more than one temperature.

[b] Strength of interaction between residues 12 and 14.

[c] Impact of PEGylation on the strength of the interaction between residues 12 and 14.